

Particle Filtering for Depth-Only Navigation on Bathymetric Maps

Rujia Li, Xinxu Yao

December 2025

1 Introduction

This project considers the problem of navigating a small boat in a lake or archipelago under extremely limited sensing conditions. The initial position of the boat is unknown, and visibility is assumed to be negligible. The only available onboard sensor is a low-quality depth gauge, while the environment is described by a known depth map. The primary objective is to infer the boat's location on the map from depth measurements alone and, once localization is sufficiently reliable, to guide the boat back to a known home position.

From a statistical perspective, this is a sequential state estimation problem with sparse and noisy observations. The hidden state consists of the boat's planar position and heading, while observations provide only indirect information through the depth field. Since the depth map is highly non-linear and spatially heterogeneous, standard linear or Gaussian filtering methods are not suitable. Instead, we adopt a particle filter, which represents the posterior distribution of the state by a cloud of weighted samples and naturally accommodates non-linearity, non-Gaussian noise, and hard spatial constraints.

An important design choice in this project is that no compass information is used. The controller does not have direct access to the true heading; instead, orientation must be inferred implicitly from the evolution of the particle cloud and the depth measurements. This setting reflects a realistic failure mode of low-cost navigation systems and places additional emphasis on internal consistency between the motion model, the map, and the measurement process.

We evaluate the proposed approach on several provided datasets. In lake environments, the method typically performs well, as spatial variations in depth provide informative measurements for localization. In contrast, the sea environment presents a more challenging case: when the seabed is relatively flat, depth measurements become less distinctive, leading to increased ambiguity and slower convergence. These limitations highlight the dependence of map-based localization on environmental variability and are discussed further in Section 6.

2 Problem Formulation and Modeling Assumptions

We formulate the navigation task as a sequential Bayesian inference problem. The objective is to infer the evolving pose of the boat from noisy depth measurements and applied control inputs, given a known depth map of the environment.

2.1 Hidden State and Observations

The hidden state at time t is defined as

$$x_t = (X_t, Y_t, \Phi_t),$$

where (X_t, Y_t) denotes the planar position of the boat and Φ_t its heading angle. The initial state x_0 is unknown.

At each time step, the only available observation is a scalar depth measurement,

$$Z_t = h(X_t, Y_t)(1 + \varepsilon_t),$$

where $h(\cdot)$ denotes the bathymetric depth map and ε_t represents relative measurement noise. According to the sensor specification, the measurement error is on the order of $\pm 15\%$. We model ε_t as a Gaussian random variable,

$$\varepsilon_t \in \mathcal{N}(0, \sigma_\varepsilon^2),$$

with $\sigma_\varepsilon = 0.1$, corresponding to a slightly conservative noise level consistent with the stated tolerance.

Since the observation depends only on the spatial position and not directly on the heading, orientation information must be inferred indirectly through the interaction between motion and depth measurements.

State evolution. The state evolves according to a stochastic motion model driven by control inputs. Let $u_t = (d_t, \Delta\phi_t)$ denote the commanded forward displacement and turning angle at time t . The state transition is given by

$$\begin{aligned} X_t &= X_{t-1} + (d_t + \eta_t^{(d)}) \cos(\Phi_{t-1} + \Delta\phi_t + \eta_t^{(\phi)}), \\ Y_t &= Y_{t-1} + (d_t + \eta_t^{(d)}) \sin(\Phi_{t-1} + \Delta\phi_t + \eta_t^{(\phi)}), \\ \Phi_t &= \Phi_{t-1} + \Delta\phi_t + \eta_t^{(\phi)}, \end{aligned}$$

where $\eta_t^{(d)}$ and $\eta_t^{(\phi)}$ represent translational and rotational noise, respectively. We also assume $\eta_t^{(d)}$ and $\eta_t^{(\phi)}$ are normally distributed, i.e. $\eta_t^{(d)} \in \mathcal{N}(0, \sigma_{\eta_d}^2)$, $\eta_t^{(\phi)} \in \mathcal{N}(0, \sigma_{\eta_\phi}^2)$. These terms capture unmodeled effects such as wind, currents, actuation variability, and control imprecision. σ_{η_d} and σ_{η_ϕ} are two hyperparameter in this model.

2.2 Why Particle Filtering Is Natural in This Setting

Before introducing algorithmic details, it is useful to explain why a particle-based approach is a natural modeling choice in this problem.

At the start of the mission, the boat has almost no information about its location or orientation. A single depth measurement only indicates that the boat lies somewhere on the map where the depth is similar to the measured value, which typically corresponds to multiple spatially separated regions rather than a unique location.

As the boat moves and collects additional depth measurements, each candidate location implies a different sequence of expected depths. Some hypotheses remain consistent with the observations, while others become increasingly implausible. Localization can therefore be viewed as maintaining and updating a set of competing hypotheses about the boat's pose.

This reasoning suggests representing uncertainty not by a single estimate with an error bar, but by a collection of possible poses, each associated with a degree of plausibility. Particle filtering implements exactly this idea by maintaining a weighted set of hypotheses that can evolve over time as new data become available.

The need for such a representation is particularly evident because uncertainty in this problem is inherently multi-modal. At intermediate stages, several distinct location hypotheses may be supported simultaneously, especially in environments where the depth map contains repeated or slowly varying structures. Particle filtering allows these multiple explanations to coexist until sufficient information becomes available to resolve the ambiguity.

Finally, orientation must also be inferred implicitly. Since depth measurements provide no direct information about heading, particles that share similar positions but differ in orientation lead to different future depth predictions. Maintaining a joint distribution over position and heading is therefore essential.

2.3 Motion Model and Physical Feasibility

In addition to stochasticity, the motion of the boat is subject to hard physical constraints imposed by the environment. In particular, the boat can only occupy positions within the navigable water domain defined by the depth map. States corresponding to land or locations outside the mapped region are physically infeasible.

This implies that the support of the state transition model is restricted to a subset of the planar domain. Inference methods that ignore this constraint may assign probability mass to impossible states, leading to misleading likelihood evaluations and unnecessary particle depletion.

When an intended movement would result in an infeasible position, the actual outcome differs qualitatively from unconstrained motion. Rather than advancing forward, the boat remains at its current location and undergoes a substantial change in heading, reflecting a collision or near-collision with the

shoreline. This behavior introduces non-smooth dynamics that cannot be captured by simple unconstrained motion models.

The collision handling adopted here is intentionally coarse-grained. Its purpose is not to model detailed physical interactions, but to capture the dominant effect of collisions on future observations: loss of forward progress combined with an abrupt and unpredictable change in orientation. Explicitly incorporating this structure ensures consistency between the motion model, the map, and the depth-based observation process.

3 Particle Filter Implementation and Design Choices

3.1 Particle Representation of Uncertainty

The particle filter represents uncertainty about the boat’s pose using a finite set of weighted samples. Each particle corresponds to a hypothesis about the hidden state,

$$x_t^{(i)} = (X_t^{(i)}, Y_t^{(i)}, \Phi_t^{(i)}),$$

with an associated weight $w_t^{(i)}$ reflecting its plausibility given the observations up to time t .

This representation is well suited to the present problem, where depth-only measurements frequently lead to multi-modal uncertainty. By maintaining a collection of particles, the filter can represent multiple competing hypotheses simultaneously and update their relative plausibility as new data become available.

3.2 Motion, Collision Handling, and Control Strategy

The motion of the boat is governed by the stochastic state evolution model described in Section 2, but is further shaped by hard physical constraints and a simple control strategy. These elements determine the sequence of states on which the particle filter operates.

Collision handling. At each time step, a tentative movement is generated based on the commanded control input and motion noise. The resulting position is then checked against the depth map. If the proposed position lies within the navigable water domain, the movement is accepted. If it is infeasible, a collision or near-collision event is assumed to occur. In this case, the boat remains at its previous location and undergoes a substantial change in heading. This mechanism captures the dominant qualitative effect of shoreline interactions: loss of forward progress combined with an abrupt and unpredictable reorientation.

Control strategy. The boat follows a simple two-phase control strategy with a fixed switching time. During an initial exploration phase, it executes a predefined circular motion pattern that does not rely on accurate localization. This

phase is designed to collect informative depth measurements under minimal assumptions about the current state estimate.

After a fixed number of time steps, the control strategy switches to a navigation phase in which the boat is steered toward the known home location using the current estimate provided by the particle filter. The switching time is chosen a priori and does not depend on any explicit convergence criterion.

This design choice reflects the fact that the information content of depth measurements depends strongly on the trajectory taken. In particular, exploratory circular motion may remain confined to regions with weak depth variation, leading to slow convergence. Steering toward the home location often results in a qualitatively different trajectory that traverses new depth gradients and can significantly accelerate localization. Importantly, localization and navigation are not treated as separate stages: the particle filter continues to update the posterior distribution throughout the navigation phase, and state estimates may continue to improve even after the switch.

Interaction with particle propagation. Throughout both phases, the particle filter remains fully active. Particles are propagated using the same control inputs applied to the boat, together with stochastic perturbations and physical feasibility checks. When collisions occur, particles are subject to the same structural constraints as the true system. As a result, the particle cloud evolves in a manner that remains consistent with the realized motion, allowing localization to be refined continuously as the boat moves.

3.3 Reducing Model Mismatch and Resampling

During collision events, the realized change in orientation may differ substantially from the commanded input. Propagating particles based solely on commands would therefore introduce systematic model mismatch. To mitigate this effect, particles are updated using odometry information reflecting the realized change in orientation, reducing divergence between the particle cloud and the true state.

Particle filters are also susceptible to weight degeneracy, where a small number of particles dominate the posterior approximation. This is monitored using the effective sample size (ESS). When the ESS falls below a predefined threshold, resampling is performed to maintain a faithful approximation of the posterior.

In rare cases of severe mismatch or uninformative observations, nearly all particles may receive negligible likelihood. In such situations, the particle cloud is reinitialized in regions consistent with the observed depth, injecting prior mass back into plausible areas of the state space.

Together, these mechanisms stabilize the inference process under challenging conditions. Odometry-aware propagation reduces systematic bias, while resampling and reinitialization prevent numerical degeneration, ensuring robust approximate Bayesian inference in constrained and weakly informative settings.

3.4 Design Parameters

The particle filter involves several design parameters that control the resolution of the posterior approximation and the robustness of the inference procedure. Before detailing the particle filter implementation, it is useful to clarify the roles of different parameters used throughout the model. Parameters introduced in Section 2 describe the stochastic data-generating process, including physical motion variability and measurement noise. In contrast, the parameters introduced in this section govern the behavior of the particle filter itself, such as the spread of the proposal distribution, the resolution of the particle approximation, and numerical stability criteria. These algorithmic parameters do not represent additional physical noise, but rather encode modeling uncertainty and computational design choices. These parameters are fixed throughout the experiments and are chosen to balance computational cost and estimation accuracy.

Number of particles. The number of particles is set to $N = 5000$. This choice reflects the high degree of uncertainty and potential multi-modality induced by depth-only measurements. A relatively large particle set is necessary to adequately represent multiple competing location hypotheses, especially during the early stages of localization.

Propagation uncertainty. During particle propagation, stochastic perturbations are introduced in both translation and rotation. The corresponding standard deviations, σ_{xy} and σ_ϕ , define the spread of the proposal distribution rather than additional physical noise. These parameters control how much deviation from the nominal motion is considered plausible and are chosen to be sufficiently large to maintain coverage of the true state under model uncertainty.

Measurement error specification. The parameter `sensorErrorSpec` controls the assumed scale of measurement uncertainty in the depth likelihood. It is chosen to be consistent with the relative error range specified for the depth sensor and serves to regularize the weight update in regions where depth measurements are weakly informative.

Resampling threshold. Weight degeneracy is monitored using the effective sample size (ESS). Resampling is triggered when the ESS falls below a fraction of the total number of particles, here set to $0.5N$. This threshold is commonly used in practice and provides a balance between avoiding premature resampling and preventing excessive weight concentration.

4 Experimental Results in Lakes

This section presents the results of the particle-filter-based localization and navigation experiments in lakes. All experiments are conducted in simulation using

the same parameter settings, and performance is evaluated across multiple lake environments with different bathymetric characteristics.

4.1 Experimental Setup

Table 1 summarizes the simulation and particle filter parameters used throughout all experiments in this section. Unless otherwise stated, these settings are kept fixed across different environments and runs.

Table 1: Simulation and particle filter parameters used in all experiments

| Category | Parameter | Value |
|-----------------|-------------------------------------------------|--------|
| Simulation | Total time steps (T) | 2500 |
| Simulation | Exploration–navigation switch step | 500 |
| Simulation | Docking radius | 5.0 |
| Simulation | Snapshot interval | 250 |
| Simulation | Water threshold | -0.3 |
| Controller | Nominal cruising speed | 0.6 |
| Controller | Reduced speed near home | 0.3 |
| Controller | Maximum steering angle | 30° |
| Motion noise | Translational noise std. ($\sigma_{xy,act}$) | 0.05 |
| Motion noise | Rotational noise std. ($\sigma_{\phi,act}$) | 1° |
| Measurement | Relative depth noise ratio | 0.10 |
| Particle filter | Number of particles (N) | 5000 |
| Particle filter | Propagation std. in position (σ_{xy}) | 0.20 |
| Particle filter | Propagation std. in heading (σ_{ϕ}) | 3° |
| Particle filter | Measurement error scaling | 0.20 |
| Particle filter | ESS resampling threshold | $0.5N$ |

4.2 Representative Successful Runs

We first present representative successful runs on three lake environments: Vombsjon, Bolmen, and Ringsjon. Each run is visualized using the figures that shows the bathymetric map together with the true trajectory, particle cloud snapshots, the estimated position, and the home location. For the first example, we add a second figure that shows the evolution of the localization error over time.

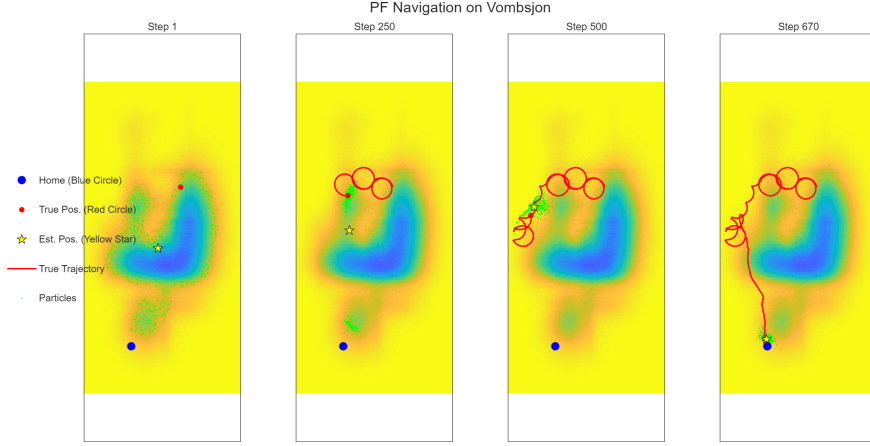


Figure 1: Successful run on Lake Vombsjon.

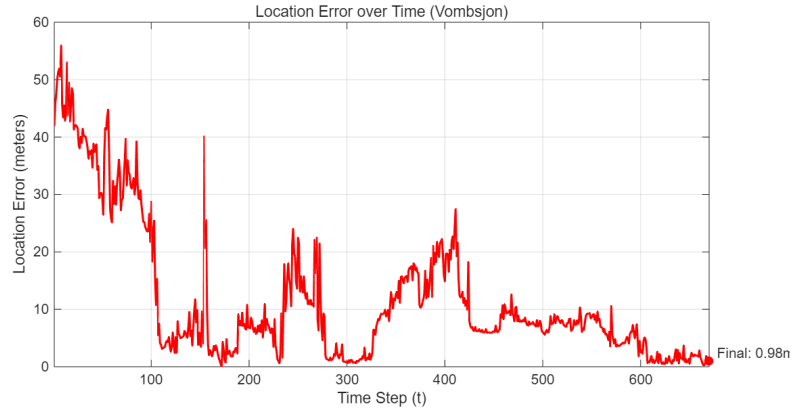


Figure 2: Localization error over time for the successful run on Lake Vombsjon.

Figure 1 and figure 2 illustrate a successful run on Lake Vombsjon. Starting from an unknown location, the particle cloud is initially widely spread, reflecting substantial uncertainty. During the exploration phase, particles gradually concentrate as depth measurements rule out incompatible regions. After the fixed switching time, the control strategy steers the boat toward the home location. The particle filter remains active throughout this phase, and the estimated position continues to improve as new depth information becomes available.

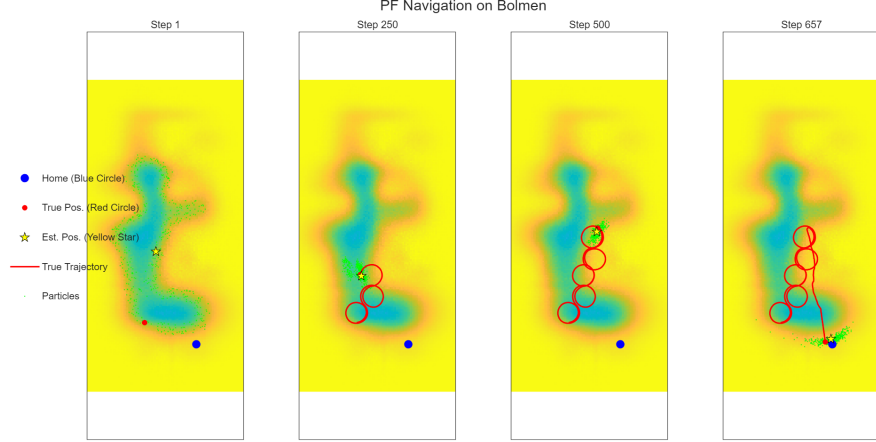


Figure 3: Successful run on Lake Bolmen.

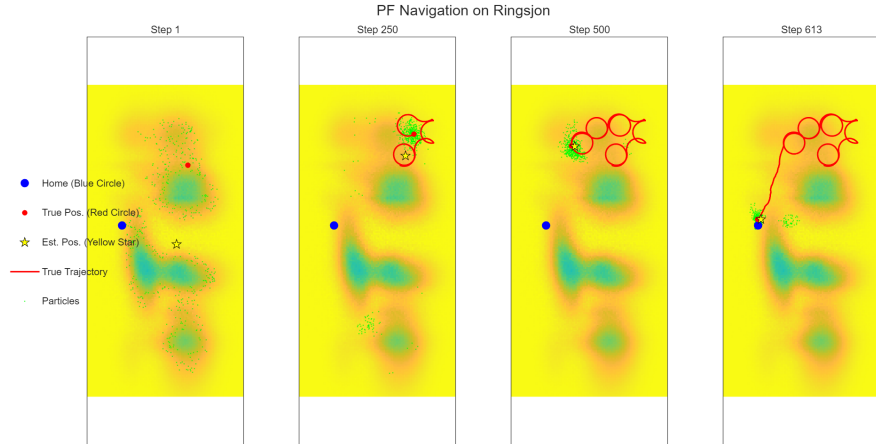


Figure 4: Successful run on Lake Ringsjon.

Similar qualitative behavior is observed in the experiments on Lake Bolmen and Lake Ringsjon (Figures 3 and 4). In all three environments, successful localization is characterized by a gradual collapse of the particle cloud onto a single dominant region, followed by stable tracking of the true trajectory during navigation.

4.3 Representative Failure Cases

We next present three representative failure cases, each illustrating a distinct limitation of the proposed navigation and localization framework. These examples highlight failure modes that arise not from implementation errors, but

from fundamental ambiguities in the sensing and control setup. Importantly, such failures are relatively rare in our experiments: across extensive simulations in multiple lake environments, the proposed method exhibits stable and reliable behavior in the vast majority of runs.

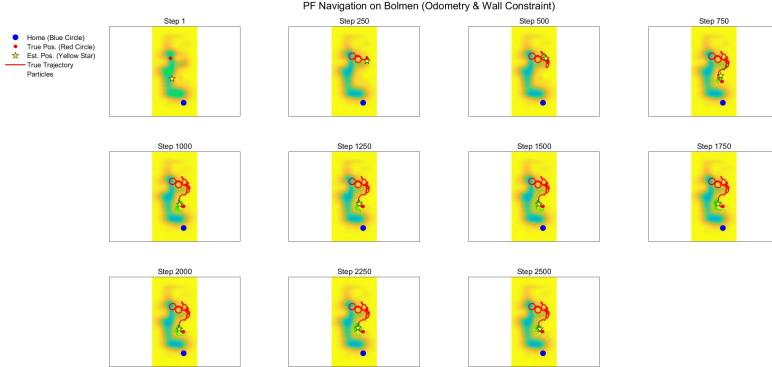


Figure 5: Failure run on Lake Bolmen.

The first failure case, shown in Figure 5, is caused by grounding (stranding) in shallow water. In this run, the boat eventually attempts a move whose proposed position lies in a non-navigable region (depth above the water threshold). The physical layer therefore rejects the translation: the true position remains unchanged while the heading undergoes a large bounce-like rotation. This creates a structural model mismatch for the particle filter. While the odometry-aware update correctly injects the large measured turn into the particles, the filter still applies a forward translation of approximately d_{cmd} in prediction. As a result, many particles repeatedly propose moves into land and get rolled back by the wall constraint, leading to a degenerate prediction step that fails to represent the true “stuck” dynamics. With the true trajectory immobilized near the boundary, depth measurements become nearly constant and provide limited information to recover from this mismatch. Consequently, the estimated position drifts, and the controller continues issuing commands that do not resolve the grounding situation, resulting in persistent failure.

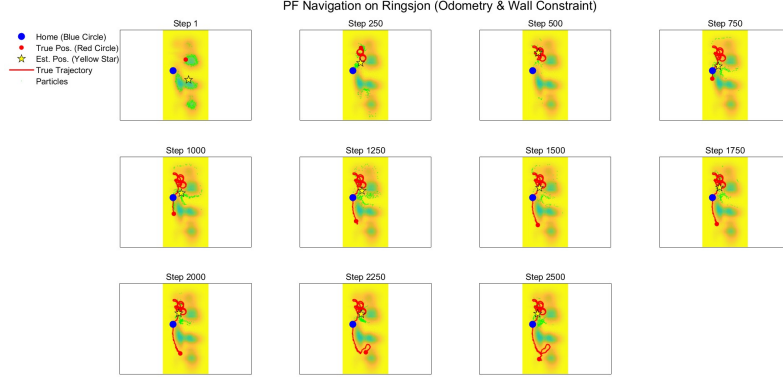


Figure 6: Failure run on Lake Ringsjon.

The second failure case, illustrated in Figure 6, demonstrates a different mechanism related to aggressive interaction with environmental boundaries. In this scenario, repeated wall collisions induce frequent and abrupt heading changes in the true trajectory. Although the odometry-aware update allows particles to track large orientation changes, the resulting motion becomes highly non-smooth. This behavior reduces the effectiveness of depth measurements, as successive observations are taken from spatially clustered locations near the boundary. Consequently, the particle cloud remains fragmented and fails to concentrate around a single dominant hypothesis, preventing reliable convergence before navigation toward the home location begins.

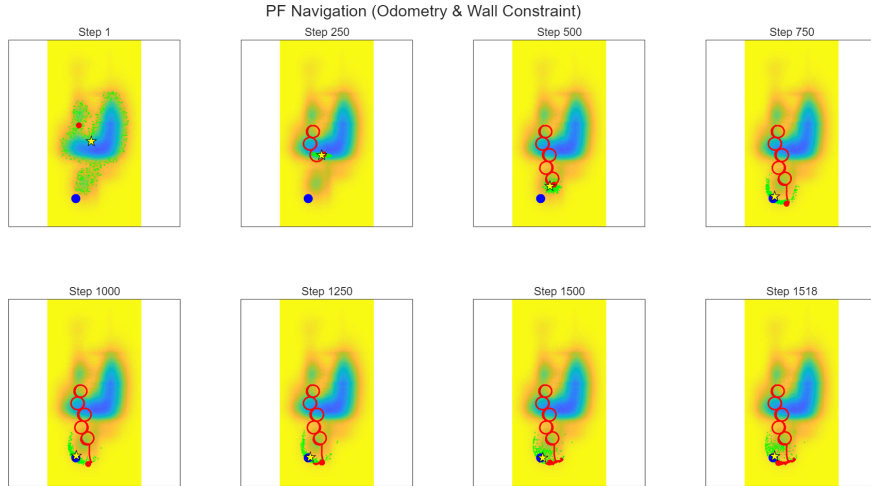


Figure 7: Failure run on Lake Ringsjon.

The third failure case, shown in Figure 7, highlights a limitation arising from strong symmetry in the bathymetric map. Here, two spatially distant regions share nearly identical depth profiles over extended areas. During exploration, particles split into two persistent modes corresponding to these regions. Despite continued filtering, neither hypothesis is decisively eliminated, resulting in a multi-modal belief that violates the unimodality implicitly assumed by the controller. When the control switches to goal-directed navigation, the estimated position reflects a compromise between modes, causing the controller to issue inconsistent commands and ultimately fail to reach the home location.

Together, these failure cases demonstrate that the proposed approach is most vulnerable in environments with strong bathymetric symmetries, limited depth gradients, or prolonged boundary-following behavior. Importantly, these scenarios indicate intrinsic limitations of depth-only sensing combined with particle filtering, rather than deficiencies of the wall-aware or odometry-aware extensions themselves. Addressing these failure modes would likely require additional sensing modalities, adaptive exploration strategies, or explicit multi-hypothesis planning mechanisms.

5 Experimental Results in the Ocean

We now turn to experiments conducted in an open ocean environment, where the bathymetric structure differs substantially from that of enclosed lakes. In contrast to the previous experiments, no parameters are retuned or adapted for this setting: the controller, motion model, and particle filter parameters are kept identical to those in Table 1.

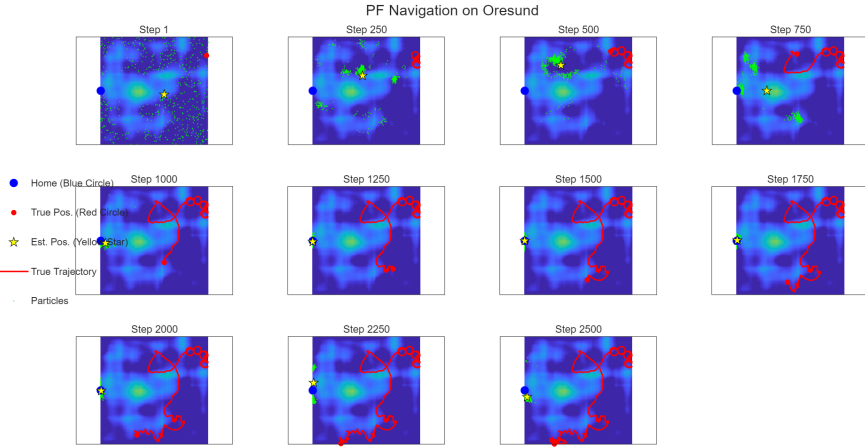


Figure 8: Failure run on Oresund.

Figure 8 presents a representative run in the Oresund environment under this unchanged configuration. Unlike the lake scenarios, the method fails to achieve

reliable localization and navigation toward the home location. This example is intentionally chosen to illustrate a typical failure mode rather than an extreme or pathological case.

The failure in this scenario can be attributed to a fundamental mismatch between the assumptions implicit in the parameter configuration and the characteristics of the ocean environment. In particular, the bathymetric map in the Oresund region exhibits relatively smooth depth variations over large spatial scales, with fewer distinctive local features compared to the lake environments. As a result, depth-only measurements provide significantly weaker localization cues, and large regions of the map remain indistinguishable under the measurement model.

During the exploration phase, the particle cloud does not collapse decisively onto a single dominant region. Instead, particles remain spread across multiple plausible hypotheses that are consistent with the observed depth values. When the controller switches to goal-directed navigation, this residual uncertainty leads to unreliable heading estimates and inconsistent control commands. The particle filter is therefore unable to track the true trajectory, and the estimated position drifts away from the ground truth despite continued filtering.

This observation suggests that successful deployment in open ocean environments requires a different balance between exploration, motion scale, and measurement uncertainty. In the following experiments, we therefore investigate how adapting a small number of key parameters—such as the nominal cruising speed, exploration duration, and particle propagation noise—can restore reliable localization and navigation performance in the ocean setting.

5.1 Parameter Adaptation for Ocean Environments

Motivated by the failure observed under the lake-tuned configuration, we next adapt a small number of parameters to account for the substantially larger spatial scale and weaker bathymetric structure of the ocean environment. Importantly, the overall algorithmic structure remains unchanged; only parameters related to scale and uncertainty are modified.

First, we increase the total simulation horizon from $T = 2500$ to $T = 3500$ and delay the exploration–navigation switch from 500 to 1000 time steps. This change reflects the fact that, in large-scale ocean maps, depth-only measurements provide weaker localization cues and require a longer exploration phase before sufficient information is accumulated to support reliable goal-directed navigation.

Second, the number of particles is increased from $N = 5000$ to $N = 20000$. In contrast to lake environments, where bathymetric features are highly distinctive and rapidly eliminate inconsistent hypotheses, the ocean setting exhibits broad regions with similar depth profiles. A larger particle set is therefore required to maintain adequate coverage of the state space and to prevent premature loss of plausible hypotheses during exploration.

Finally, we increase the nominal cruising speed during exploration while keeping the reduced speed near the home location and the steering limits un-

changed. This adjustment effectively enlarges the spatial footprint of exploratory motion, allowing the vehicle to traverse larger areas and encounter more diverse bathymetric features within a fixed number of time steps. In large-scale environments, such increased exploratory motion is essential for breaking depth ambiguities that cannot be resolved through small, localized movements.

Overall, these modifications can be interpreted as a uniform rescaling of temporal, spatial, and probabilistic resolution to match the characteristics of the ocean environment. No additional sensing modalities or algorithmic components are introduced, demonstrating that the proposed framework remains applicable beyond lake settings when its parameters are scaled appropriately.

Table 2: Comparison of parameter settings for lake and ocean environments

| Category | Parameter | Lakes | Ocean |
|-----------------|-------------------------------------------------|--------|--------|
| Simulation | Total time steps (T) | 2500 | 3500 |
| Simulation | Exploration–navigation switch step | 500 | 1000 |
| Simulation | Docking radius | 5.0 | 5.0 |
| Simulation | Snapshot interval | 250 | 250 |
| Controller | Nominal cruising speed | 0.6 | 1.2 |
| Controller | Reduced speed near home | 0.3 | 0.3 |
| Controller | Maximum steering angle | 30° | 30° |
| Motion noise | Translational noise std. ($\sigma_{xy,act}$) | 0.05 | 0.05 |
| Motion noise | Rotational noise std. ($\sigma_{\phi,act}$) | 1° | 1° |
| Measurement | Relative depth noise ratio | 0.10 | 0.10 |
| Particle filter | Number of particles (N) | 5000 | 20000 |
| Particle filter | Propagation std. in position (σ_{xy}) | 0.20 | 0.20 |
| Particle filter | Propagation std. in heading (σ_{ϕ}) | 3° | 3° |
| Particle filter | Measurement error scaling | 0.20 | 0.20 |
| Particle filter | ESS resampling threshold | $0.5N$ | $0.5N$ |

5.2 Successful Navigation after Parameter Rescaling

We now demonstrate that the proposed parameter rescaling is sufficient to restore reliable localization and navigation performance in open ocean environments. Figures 9 and 10 show representative successful runs in the Oresund and Skagerrak regions, respectively, using the adapted parameter configuration summarized in Table 2.

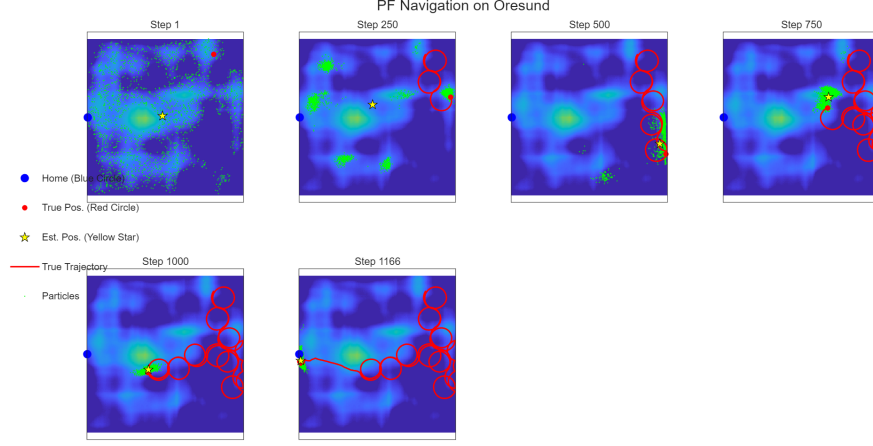


Figure 9: Successful run on Oresund.

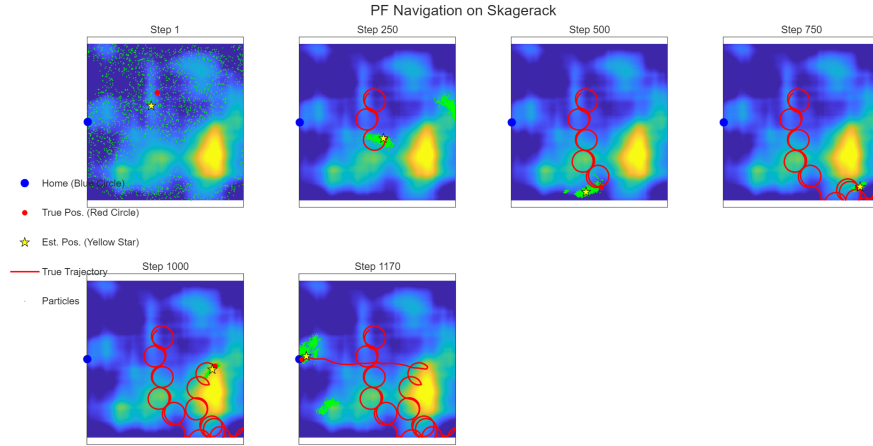


Figure 10: Successful run on Skagerack.

In both environments, the exploration phase leads to a gradual but decisive concentration of the particle cloud, despite the relatively smooth and large-scale bathymetric structure. Compared to the lake experiments, convergence occurs over a longer time horizon, reflecting the weaker informativeness of individual depth measurements. Nevertheless, the increased number of particles and extended exploration duration ensure that multiple plausible hypotheses are retained until sufficient evidence is accumulated.

After the switch to goal-directed navigation, the estimated position remains well aligned with the true trajectory, and stable tracking is maintained throughout the remainder of the run. Notably, the same control strategy and motion model used in the lake experiments are sufficient once the temporal, spatial,

and probabilistic scales are appropriately adjusted.

Discussion and Conclusion. The ocean experiments reveal a clear contrast to the lake scenarios. Even after appropriate parameter rescaling, the success rate in ocean environments remains lower than that observed in lakes. This gap is not unexpected and can be attributed to fundamental differences in the identifiability of the localization problem rather than to deficiencies in the proposed algorithm.

In lake environments, bathymetric maps typically exhibit strong local variations and distinctive features over relatively small spatial scales. As a consequence, depth-only measurements provide high information content, enabling rapid elimination of inconsistent hypotheses and robust convergence of the particle filter. In contrast, open ocean bathymetry is often smoother and more homogeneous over large regions, leading to extended areas that are nearly indistinguishable under the depth measurement model. This reduced identifiability implies that even long exploration phases may fail to fully resolve global ambiguities in the state space.

From this perspective, the lower success rate in ocean experiments reflects an intrinsic limitation of depth-only localization in weakly informative environments. Parameter rescaling—such as increasing the number of particles, extending exploration time, and enlarging the spatial footprint of exploratory motion—can partially mitigate these effects by preserving multiple hypotheses for longer durations. However, such adjustments cannot fully compensate for the lack of distinctive environmental features.

Overall, these results suggest that while the proposed framework generalizes to ocean-scale settings under appropriate parameter scaling, its ultimate performance is fundamentally constrained by the identifiability of the underlying sensing modality. Addressing this limitation would likely require either additional sensing information or exploration strategies explicitly designed to maximize information gain.

6 Conclusion

In this project, we studied the problem of autonomous navigation and localization using depth-only measurements in bathymetric environments. We proposed a particle-filter-based framework that integrates a simple exploration–navigation control strategy with odometry-aware and wall-aware motion modeling. The resulting system requires minimal sensing assumptions and relies solely on depth information and a known bathymetric map.

Through extensive simulation studies in multiple lake environments, we demonstrated that the proposed approach achieves stable and reliable localization under realistic noise and motion uncertainty. In these settings, distinctive bathymetric features provide sufficient information for the particle filter to rapidly eliminate inconsistent hypotheses, leading to accurate state estimation and successful navigation toward a home location.

We further investigated the transferability of the method to open ocean environments. When applied without modification, the lake-tuned parameter configuration leads to systematic failures, highlighting a mismatch between environmental scale and parameter assumptions. By rescaling a small number of key parameters—specifically those related to temporal horizon, spatial tolerance, and probabilistic resolution—we showed that successful localization and navigation can be recovered in ocean-scale settings without altering the underlying algorithmic structure.

Importantly, our experiments also reveal fundamental limitations of depth-only localization. Even with appropriate parameter adaptation, success rates in ocean environments remain lower than in lakes. This gap is best understood through the lens of identifiability: in large-scale and weakly structured bathymetric maps, depth measurements alone may be insufficient to uniquely determine the vehicle’s position. As a result, no amount of parameter tuning can fully compensate for a lack of informative environmental features.

Overall, this work demonstrates both the strengths and the intrinsic limits of depth-based particle-filter localization. The proposed framework offers a simple and robust solution in information-rich environments, while also serving as a concrete case study of how sensing modality and environmental structure jointly determine localization performance. Future work may explore information-aware exploration strategies or the integration of additional sensing modalities to address identifiability constraints in large-scale environments.